

# The evolution of massive black hole seeds

Marta Volonteri<sup>1</sup>, Giuseppe Lodato<sup>2</sup> & Priyamvada Natarajan<sup>3,4</sup>

<sup>\*</sup> <sup>1</sup> *Department Of Astronomy, University of Michigan, Ann Arbor, MI, USA*

<sup>2</sup> *Department of Physics and Astronomy, University of Leicester, Leicester, LE1 7RH, UK*

<sup>3</sup> *Department of Astronomy, Yale University, P. O. Box 208101, New Haven, CT 06511-208101, USA*

<sup>4</sup> *Department of Physics, Yale University, P. O. Box 208120, New Haven, CT 06520-208120, USA*

27 November 2018

## ABSTRACT

We investigate the evolution of high redshift seed black hole masses at late times and their observational signatures. The massive black hole seeds studied here form at extremely high redshifts from the direct collapse of pre-galactic gas discs. Populating dark matter halos with seeds formed in this way, we follow the mass assembly of these black holes to the present time using a Monte-Carlo merger tree. Using this machinery we predict the black hole mass function at high redshifts and at the present time; the integrated mass density of black holes and the luminosity function of accreting black holes as a function of redshift. These predictions are made for a set of three seed models with varying black hole formation efficiency. Given the accuracy of current observational constraints, all 3 models can be adequately fit. Discrimination between the models appears predominantly at the low mass end of the present day black hole mass function which is not observationally well constrained. However, all our models predict that low surface brightness, bulgeless galaxies with large discs are least likely to be sites for the formation of massive seed black holes at high redshifts. The efficiency of seed formation at high redshifts has a direct influence on the black hole occupation fraction in galaxies at  $z = 0$ . This effect is more pronounced for low mass galaxies. This is the key discriminant between the models studied here and the Population III remnant seed model. We find that there exists a population of low mass galaxies that do not host nuclear black holes. Our prediction of the shape of the  $M_{\text{bh}} - \sigma$  relation at the low mass end is in agreement with the recent observational determination from the census of low mass galaxies in the Virgo cluster.

**Key words:**

## 1 INTRODUCTION

The demography of local galaxies suggests that most galaxies host a quiescent supermassive black hole (SMBH) at the present time and the properties of the black hole are correlated with those of the host spheroid. In particular, recent observational evidence points to the existence of a tight correlation between the mass of the central black hole and the velocity dispersion of the host spheroid (Tremaine et al. 2002; Ferrarese & Merritt 2000; Gebhardt et al. 2000) in nearby galaxies. This correlation strongly suggests coeval growth of the black hole and the stellar component via likely regulation of the gas supply in galactic nuclei (Silk & Rees 1998; Kauffmann & Haehnelt 2000; King 2003; Thompson et al. 2005).

Black hole growth is believed to be powered by gas accretion (Lynden-Bell 1969) and accreting black holes are detected as optically bright quasars. These optically bright quasars appear to exist out to the highest redshifts probed at the present time. Therefore, the mass build-up of SMBHs

is likely to have commenced at extremely high redshifts ( $z > 10$ ). In fact, optically bright quasars have now been detected at  $z > 6$  (e.g., Fan et al. 2004; Fan et al. 2006) in the Sloan Digital Sky Survey (SDSS). Hosts of high redshift quasars are often strong sources of dust emission (Omont et al. 2001; Cox et al. 2002; Carilli et al. 2002; Walter et al. 2003), suggesting that quasars were already in place in massive galaxies at a time when galaxies were undergoing vigorous star formation. The growth spurts of SMBHs are also seen in the X-ray waveband. The integrated emission from these X-ray quasars generates the cosmic X-ray background (XRB), and its spectrum suggests that most black-hole growth is obscured in optical wavelengths (Fabian & Iwasawa 1999; Mushotzky et al. 2000; Hasinger et al. 2001; Barger et al. 2003, 2005; Worsley et al. 2005). There exist examples of obscured black-hole growth in the form of ‘Type-2’ quasars, but their detected numbers are fewer than expected from models of the XRB. However, there is recent tantalizing evidence from infra-red (IR) studies that dust-obscured ac-

tion is ubiquitous (Martínez-Sansigre et al. 2005). Current work suggests that while SMBHs might spend most of their lifetime in an optically dim phase, the bulk of mass growth occurs in the short-lived quasar stages.

The assembly of BH mass in the Universe has been tracked using optical quasar activity. The current phenomenological approach to understanding the assembly of SMBHs involves optical data from both high and low redshifts. These data are used as a starting point to construct a consistent picture that fits within the larger framework of the growth and evolution of structure in the Universe (Haehnelt et al. 1998; Haiman & Loeb 1998; Kauffmann & Haehnelt 2000, 2002; Wyithe & Loeb 2002; Volonteri et al. 2003; Di Matteo et al. 2003).

Current modeling is grounded in the framework of the standard paradigm that involves the growth of structure via gravitational amplification of small perturbations in a CDM Universe—a model that has independent validation, most recently from *Wilkinson Microwave Anisotropy Probe* (WMAP) measurements of the anisotropies in the cosmic microwave background (Spergel et al. 2003; Page et al. 2003). Structure formation is tracked in cosmic time by keeping a census of the number of collapsed dark matter halos of a given mass that form; these provide the sites for harboring black holes. The computation of the mass function of dark matter halos is done using either the Press-Schechter (Press & Schechter 1974) or the extended Press-Schechter theory (Lacey & Cole 1993), or Monte-Carlo realizations of merger trees (Kauffmann & Haehnelt 2000; Volonteri et al. 2003; Bromley et al. 2004) or, in some cases, directly from cosmological N-body simulations (Di Matteo et al. 2003, 2005).

In particular Volonteri et al. (2003) have presented a detailed merger-tree based scenario to trace the growth of black holes from the earliest epochs to the present day. Monte-Carlo merger trees are created for present day halos and propagated back in time to a redshift of  $\sim 20$ . With the merging history thus determined, the initial halos at  $z \sim 20$  are then populated with seed black holes which are assumed to be remnants of the first stars that form in the Universe. The masses of these so-called Population III stars are not accurately known, however numerical simulations by various groups (Abel et al. 2000; Bromm et al. 2002) suggest that they are skewed to high masses of the order of a few hundred solar masses. Seeded with the end products of this first population, the merger sequence is followed and black holes are assumed to grow with every major merger episode. An accretion episode is assumed to occur as a consequence of every merger event. Following the growth and mass assembly of these black holes, it is required that the model is in consonance with the observed local  $M_{\text{BH}} - \sigma$  relation. The luminosity function of quasars is predicted by these models and can be compared to observations. Volonteri et al. find that not every halo at high redshift needs to be populated with a black hole seed in order to satisfy the observational constraints at  $z = 0$ . These models do not automatically reproduce the required abundance of supermassive black holes inferred to power the observed  $z > 6$  SDSS quasars. In order to match the observation and produce SMBHs roughly 1 Gyr after the Big Bang, it is required that black holes undergo brief, but extremely strong growth episodes during which the accretion rate onto them is well in excess of

the Eddington rate (Volonteri & Rees 2005; Begelman et al. 2006). It is the existence of these SMBHs powering quasars at  $z > 6$  that has prompted work on alternate channels to explain their mass build-up.

In order to alleviate the problem of explaining the existence of SMBHs in place by  $z \sim 6$ , roughly 1 Gyr after the Big Bang, in this paper we examine the possibility of using a well motivated high redshift seed black hole mass function as the initial black hole population at the highest redshifts. We investigate the effect of populating early dark matter halos with massive black hole seeds predicted in a model proposed by Lodato & Natarajan (2006, 2007). This model predicts a mass function for black holes that results from the direct collapse of pre-galactic gas discs. We study the implications of the use of this seed mass function versus that of the Population III remnants, in particular the difference in predictions at  $z = 0$  for the massive seed models. In Section 2, we briefly outline the high redshift BH seed formation model, in Section 3 we evolve this model with redshift using the merger-tree formalism developed by Volonteri et al. (2003). The results are presented in Section 4, followed by a discussion of implications in the final section.

## 2 BH SEED FORMATION MODEL

In this paper, we track the formation of seed black holes in an ab-initio model and follow their mass assembly down to  $z = 0$ . This is done in two separate phases - starting with the high redshift seeds and tracing their subsequent growth. At high redshift ( $z > 15$ ), we assume the intergalactic medium has not been significantly enriched by metals, and therefore the gas cooling timescales are long. Under these conditions, many authors (Koushiappas et al. 2004; Begelman et al. 2006; Lodato & Natarajan 2006, 2007) have shown that pre-galactic discs can efficiently transport matter into their innermost regions through the development and amplification of non-axisymmetric gravitational instabilities, often without fragmentation and star formation taking place (see below). This is the main seed formation phase, wherein massive seeds with  $M \approx 10^5 - 10^6 M_{\odot}$  can form. At lower redshifts, cooling becomes more efficient and we assume that further accretion occurs via a ‘merger driven scenario’ described in more detail in Section 3. In this section we provide simple, analytical estimates of the amount of mass that we expect to be assembled in the form of massive BH seeds, based on the above scenario, as a function of the key dark matter halo parameters. Here we refer in particular to the model by Lodato & Natarajan (2006), who considered the evolution of pre-galactic discs by self-consistently taking into account gravitational stability and fragmentation, thereby providing a detailed inventory of the fate of the gas.

Consider a dark matter halo of mass  $M$  and virial temperature  $T_{\text{vir}}$ , containing gas mass  $M_{\text{gas}} = m_{\text{d}}M$  (we also assume that the baryon fraction is roughly 5% implying  $m_{\text{d}} = 0.05$ ), of primordial composition, i.e. gas not enriched by metals, for which the cooling function is dominated by hydrogen. The other main parameter characterizing a dark matter halo that is relevant to the fate of the gas is its spin parameter  $\lambda$  ( $\equiv J_h E_h^{1/2} / GM_h^{5/2}$ , where  $J_h$  is the total angular momentum and  $E_h$  is the binding energy). The distribution of spin parameters for dark matter halos measured

in numerical simulations is well fit by a lognormal distribution in  $\lambda_{\text{spin}}$ , with mean  $\bar{\lambda}_{\text{spin}} = 0.05$  and standard deviation  $\sigma_\lambda = 0.5$ :

$$p(\lambda) d\lambda = \frac{1}{\sqrt{2\pi}\sigma_\lambda} \exp\left[-\frac{\ln^2(\lambda/\bar{\lambda})}{2\sigma_\lambda^2}\right] \frac{d\lambda}{\lambda}, \quad (1)$$

This function has been shown to provide a good fit to the N-body results of several investigations (e.g., Warren et al. 1992; Cole & Lacey 1996; Bullock et al. 2001; van den Bosch et al. 2002).

If the virial temperature of the halo  $T_{\text{vir}} > T_{\text{gas}}$ , the gas collapses and forms a rotationally supported disc. For low values of the spin parameter  $\lambda$  the resulting disc can be compact and dense and is subject to gravitational instabilities. This occurs when the stability parameter  $Q$  defined below approaches unity:

$$Q = \frac{c_s \kappa}{\pi G \Sigma} = \sqrt{2} \frac{c_s V_h}{\pi G \Sigma R}, \quad (2)$$

where  $R$  is the cylindrical radial coordinate,  $\Sigma$  is the surface mass density,  $c_s$  is the sound speed,  $\kappa = \sqrt{2}V_h/R$  is the epicyclic frequency, and  $V_h$  is the circular velocity of the disc (mostly determined by the dark matter gravitational potential). We have also assumed that at the relevant radii ( $\approx 10^2 - 10^3$  pc) the rotation curve is well described by a flat  $V_h$  profile. We consider here the earliest generations of gas discs, which are of pristine composition with no metals and therefore can cool only via hydrogen. In thermal equilibrium, if the formation of molecular hydrogen is suppressed, these discs are expected to be nearly isothermal at a temperature of a few thousand Kelvin (here we take  $T_{\text{gas}} \approx 5000\text{K}$ , Lodato & Natarajan 2006). However, molecular hydrogen if present can cool these discs further down to temperatures of a few hundred Kelvin. The stability parameter has a critical value  $Q_c$  of the order of unity, below which the disc is unstable leading to the potential formation of a seed black hole. The actual value of  $Q_c$  essentially determines how stable the disc is, with lower  $Q_c$ 's implying more stable discs. It is well known since Toomre (1964) proposed this stability criterion, that for an infinitesimally thin disc to be stable to fragmentation,  $Q_c = 1$  for axisymmetric disturbances. The exact value of  $Q_c$  under more realistic conditions is not well determined. Finite thickness effects tend to stabilize the disc (reducing  $Q_c$ ), while on the other hand non-axisymmetric perturbations are in reality more unstable (enhancing  $Q_c$ ). Global, three-dimensional simulations of Keplerian discs (Lodato & Rice 2004, 2005) have shown that such discs settle down in a quasi-equilibrium configuration with  $Q$  remarkably close to unity, implying that the critical value  $Q_c \approx 1$ . In this paper, we take  $Q_c$  to be a free parameter and evaluate our results for a range of values.

If the disc becomes unstable it develops non-axisymmetric spiral structures, which leads to an effective redistribution of angular momentum, thus feeding a growing seed black hole in the center. This process stops when the amount of mass transported to the center,  $M_{\text{BH}}$ , is enough to make the disc marginally stable. This can be computed easily from the stability criterion in eqn. (2) and from the disc properties, determined from the dark matter halo mass and angular momentum (Mo et al. 1998). In this way we obtain that the mass accumulated in the center of the halo is given by:

$$M_{\text{BH}} = \begin{cases} m_d M \left[ 1 - \sqrt{\frac{8\lambda}{m_d Q_c} \left(\frac{j_d}{m_d}\right) \left(\frac{T_{\text{gas}}}{T_{\text{vir}}}\right)^{1/2}} \right] & \lambda < \lambda_{\text{max}} \\ 0 & \lambda > \lambda_{\text{max}} \end{cases} \quad (3)$$

where

$$\lambda_{\text{max}} = m_d Q_c / 8 (m_d / j_d) (T_{\text{vir}} / T_{\text{gas}})^{1/2} \quad (4)$$

is the maximum halo spin parameter for which the disc is gravitationally unstable. Note that while  $Q_c = 1$  provides the benchmark for the onset of instability, non-axisymmetric and global instabilities can cause the disc to become unstable for larger values of  $Q_c$ . For this reason we investigate models with  $1 < Q_c \leq 3$ .

The process described above provides a means to transport matter from a typical scale of a few hundred parsecs down to radii of a few AU. If the halo-disc system already possesses a massive black hole seed from a previous generation, then this gas can provide a large fuel reservoir for its further growth. Note that the typical accretion rates implied by the above model are of the order of  $0.01 M_\odot/\text{yr}$ , and are therefore sub-Eddington for seeds with masses of the order of  $10^5 M_\odot$  or so. If, on the other hand no black hole seed is present, then this large gas inflow can form a seed anew. The ultimate fate of the gas in this case at the smallest scales is more uncertain. One possibility, if the accretion rate is sufficiently large, has been described in detail by Begelman et al. (2006). The infalling material likely forms a quasi-star, the core of which collapses and forms a BH, while the quasi-star keeps accreting and growing in mass at a rate which would be super-Eddington for the central BH. Alternatively, the gas might form a super-massive star, which would eventually collapse and form a black hole (Shapiro & Shibata 2002). There are no quantitative estimates of how much mass would ultimately end up collapsing in the hole. Thus, the black hole seed mass estimates based on eqn. 3 should be considered as upper limits.

For large halo mass, the internal torques needed to redistribute the excess baryonic mass become too large to be sustained by the disc, which then undergoes fragmentation. This occurs when the virial temperature exceeds a critical value  $T_{\text{max}}$ , given by:

$$\frac{T_{\text{max}}}{T_{\text{gas}}} > \left( \frac{4\alpha_c}{m_d} \frac{1}{1 + M_{\text{BH}}/m_d} \right)^{2/3}, \quad (5)$$

where  $\alpha_c \approx 0.06$  is a dimensionless parameter measuring the critical gravitational torque above which the disc fragments (Rice et al. 2005).

To summarize, every dark matter halo is characterized by its mass  $M$  (or virial temperature  $T_{\text{vir}}$ ) and by its spin parameter  $\lambda$ . The gas has a temperature  $T_{\text{gas}} = 5000\text{K}$ . If  $\lambda < \lambda_{\text{max}}$  (see eqn. 4) and  $T_{\text{vir}} < T_{\text{max}}$  (eqn. 5), then we assume that a seed BH of mass  $M_{\text{BH}}$  given by eqn. (3) forms in the center. The remaining relevant parameters are  $m_d = 0.05$ ,  $\alpha_c = 0.06$ , and we consider three different values for  $Q_c = 1.5, 2, 3$ , which will be referred to as (i) model A; (ii) model B and (iii) model C which correspond respectively to cases of increasing instability and therefore increasing efficiency for the formation of seed black holes. What we investigate in this paper are possible constraints/insights that the measured mass function of supermassive black holes at  $z = 0$  can provide on the onset of instability and therefore on the efficiency of seed formation at extremely high redshifts.

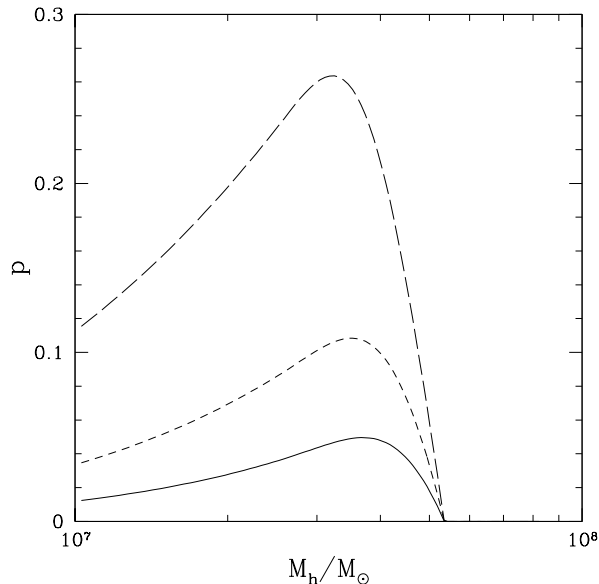


**Figure 1.** The probability of hosting a BH seed of any mass at  $z = 18$  as a function of dark matter halo mass. The three curves refer to  $Q_c = 1.5$  (low efficiency case, solid line),  $Q_c = 2$  (intermediate efficiency, short-dashed line) and  $Q_c = 3$  (high efficiency, long-dashed line).

To give an idea of the efficiency of BH seed formation at high  $z$  within the present model, we plot in Fig. 1, as an example, the probability of forming a BH (of any mass) at  $z = 18$ , as a function of halo mass, for the three models. It can be seen that typically up to 10% of the haloes in the right mass range can form a central seed BH, the percentage rising to a maximum of  $\approx 25\%$  for the high efficiency model C (highly unstable discs), and dropping to a maximum of  $\approx 4\%$  for the high stability and therefore low efficiency case (model A).

### 3 THE EVOLUTION OF SEED BLACK HOLES

We follow the evolution of the MBH population resulting from the seed formation process delineated above in a  $\Lambda$ CDM Universe. Our approach is similar to the one described in Volonteri, Haardt & Madau (2003). We simulate the merger history of present-day halos with masses in the range  $10^{11} < M < 10^{15} M_\odot$  starting from  $z = 20$ , via a Monte Carlo algorithm based on the extended Press-Schechter formalism.

Every halo entering the merger tree is assigned a spin parameter according to eqn. 1. Recent work on the fate of halo spins during mergers in cosmological simulations has led to conflicting results: Vitvitska et al. (2002) suggest that the spin parameter of a halo increases after a major merger, and the angular momentum decreases after a long series of minor mergers; D’Onghia & Navarro (2007) find instead no significant correlation between spin and merger history. Given the unsettled nature of this matter, we adopt Occam’s razor to guide us, and assume that the spin parameter of a halo is not modified by its merger history.

When a halo enters the merger tree we assign seed

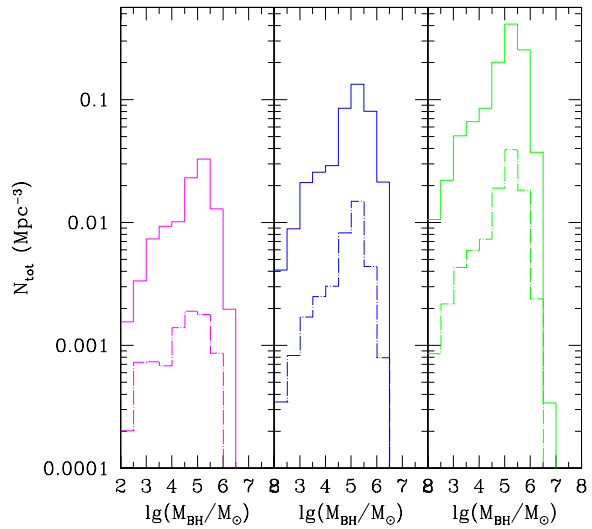


**Figure 2.** Mass function of MBH seeds in three Q-models of that differ in seed formation efficiency. Left panel:  $Q_c = 1.5$  (the least efficient model A), middle panel:  $Q_c = 2$  (intermediate efficiency model B), right panel:  $Q_c = 3$  (highly efficient model C). Seeds form at  $z > 15$  and this channel ceases at  $z = 15$ . The solid histograms show the total mass function of seeds formed by  $z = 15$ , while the dashed histograms refer to seeds formed at a specific redshift,  $z = 18$ .

MBHs by determining if the halo meets all the requirements described in Section 2 for the formation of a central mass concentration. As we do not self-consistently trace the metal enrichment of the intergalactic medium, we consider here a sharp transition threshold, and assume that the MBH formation scenario suggested by Lodato & Natarajan ceases at  $z \approx 15$  (see also Sesana et al. 2007; Volonteri 2007). At  $z > 15$ , therefore, whenever a new halo appears in the merger tree (because its mass is larger than the mass resolution), or a pre-existing halo modifies its mass by a merger, we evaluate if the gaseous component meets the conditions for efficient transport of angular momentum to create a large inflow of gas which can either form a MBH seed, or feed one if already present.

The efficiency of MBH formation is strongly dependent on critical value of the Toomre parameter  $Q_c$ , which sets the frequency of formation, and consequently the number density of MBH seeds. We investigate the influence of this parameter in the determination of the global evolution of the MBH population. Fig. 2 shows the number density of seeds formed in three models, with  $Q_c = 1.5$  (low efficiency model A),  $Q_c = 2$  (intermediate efficiency model B), and  $Q_c = 3$  (high efficiency model C). The solid histograms show the total mass function of seeds formed by  $z = 15$  when this formation channel ceases, while the dashed histograms refer to seeds formed at a specific redshift slice at  $z = 18$ . The number of seeds changes by about one order of magnitude from the least efficient to the most efficient model, consistent with the probabilities shown in Fig. 1.

We assume that, after seed formation ceases, the  $z < 15$  population of MBHs evolves according to a “merger driven

scenario”, as described in Volonteri et al. (2006). We assume that during major mergers MBHs accrete gas mass that scales with the fifth power of the circular velocity (or equivalently the velocity dispersion  $\sigma_c$ ) of the host halo (Ferrarese 2002). We thus set the final mass of the MBH at the end of the accretion episode to 90% of the mass predicted by the  $M_{\text{BH}} - \sigma_c$  correlation, assuming that the scaling does not evolve with redshift. Major mergers are defined as mergers between two dark matter halos with mass ratio between 1 and 10. BH mergers contribute to the mass increase of the remaining 10%.

In order to calculate the accreting black hole luminosity function and to follow the black hole mass growth during each accretion event, we also need to calculate the rate at which the mass, as estimated above, is accreted. This is assumed to scale with the Eddington rate for the MBH, and is based on the results of merger simulations, which heuristically track accretion onto a central MBH (Di Matteo et al. 2005; Hopkins et al. 2005a). The time spent by a given simulated AGN at a given bolometric luminosity<sup>1</sup> per logarithmic interval is approximated by (Hopkins et al. 2005b) as:

$$\frac{dt}{dL} = |\alpha| t_Q L^{-1} \left( \frac{L}{10^9 L_\odot} \right)^\alpha, \quad (6)$$

where  $t_Q \simeq 10^9$  yr, and  $\alpha = -0.95 + 0.32 \log(L_{\text{peak}}/10^{12} L_\odot)$ . Here  $L_{\text{peak}}$  is the luminosity of the AGN at the peak of its activity. Hopkins et al. (2006) show that approximating  $L_{\text{peak}}$  with the Eddington luminosity of the MBH at its final mass (i.e., when it sits on the  $M_{\text{BH}} - \sigma_c$  relation) compared to computing the peak luminosity with eqn. (6) above gives the same result and in fact, the difference between these 2 cases is negligible. Volonteri et al. (2006) derive the following simple differential equation to express the instantaneous accretion rate ( $f_{\text{Edd}}$ , in units of the Eddington rate) for a MBH of mass  $M_{\text{BH}}$  in a galaxy with velocity dispersion  $\sigma_c$ :

$$\frac{df_{\text{Edd}}(t)}{dt} = \frac{f_{\text{Edd}}^{1-\alpha}(t)}{|\alpha| t_Q} \left( \frac{\epsilon \dot{M}_{\text{Edd}} c^2}{10^9 L_\odot} \right)^{-\alpha}, \quad (7)$$

where here  $t$  is the time elapsed from the beginning of the accretion event. Solving this equation gives us the instantaneous Eddington ratio for a given MBH at a specific time, and therefore we can self-consistently grow the MBH mass. We set the Eddington ratio  $f_{\text{Edd}} = 10^{-3}$  at  $t = 0$ . This same type of accretion is assumed to occur, at  $z > 15$ , following a major merger in which a MBH is not fed by disc instabilities.

In a hierarchical Universe, where galaxies grow by mergers, MBH mergers are a natural consequence, and we trace their contribution to the evolving MBH population (cfr. Sesana et al. 2007 for details on the dynamical modeling). During the final phases of a MBH merger, emission of gravitational radiation drives the orbital decay of the binary. Recent numerical relativity simulations

suggest that merging MBH binaries might be subject to a large “gravitational recoil”: a general-relativistic effect (Fitchett 1983; Redmount & Rees 1989) due to the non-zero net linear momentum carried away by gravitational waves in the coalescence of two unequal mass black holes. Radiation recoil is a strong field effect that depends on the lack of symmetry in the system. For merging MBHs with high spin, in particular orbital configurations, the recoil velocity can be as high as a few thousands of kilometers per second (Campanelli et al. 2007a,b; González et al. 2007; Herrmann et al. 2007; Schnittman 2007). Here, we aim to determine the characteristic features of the MBH population deriving from a specific seed scenario, and its signature in present-day galaxies, we study the case without gravitational recoil. We discuss this issue further in section 4.

## 4 RESULTS

Detection of gravitational waves from seeds merging at the redshift of formation (Sesana et al. 2007) is probably one of the best ways to discriminate among formation mechanisms. On the other hand, the imprint of different formation scenarios can also be sought in observations at lower redshifts. The various seed formation scenarios have distinct consequences for the properties of the MBH population at  $z = 0$ . Below, we present theoretical predictions of the various seed models for the properties of the local SMBH population.

### 4.1 Supermassive black holes in dwarf galaxies

The repercussions of different initial efficiencies for seed formation for the overall evolution of the MBH population stretch from high-redshift to the local Universe. Obviously, a higher density of MBH seeds implies a more numerous population of MBHs at later times, which can produce observational signatures in statistical samples. More subtly, the formation of seeds in a  $\Lambda$ CDM scenario follows the cosmological bias. As a consequence, the progenitors of massive galaxies (or clusters of galaxies) have a higher probability of hosting MBH seeds (cfr. Madau & Rees 2001). In the case of low-bias systems, such as isolated dwarf galaxies, very few of the high- $z$  progenitors have the deep potential wells needed for gas retention and cooling, a prerequisite for MBH formation. We can read off directly from Fig. 1 the average number of massive progenitors required for a present day galaxy to host a MBH. In model A, a galaxy needs of order 25 massive progenitors (mass above  $\sim 10^7 M_\odot$ ) to ensure a high probability of seeding within the merger tree. In model C, instead, the requirement drops to 4 massive progenitors, increasing the probability of MBH formation in lower bias halos.

The signature of the efficiency of the formation of MBH seeds will consequently be stronger in isolated dwarf galaxies. Fig. 3 (bottom panel) shows a comparison between the observed  $M_{\text{BH}} - \sigma$  relation and the one predicted by our models (shown with circles), and in particular, from left to right, the three models based on the Lodato & Natarajan (2006, 2007) seed masses with  $Q_c = 1.5, 2$  and 3, and a fourth model based on lower-mass Population III star seeds. The upper panel of Fig. 3 shows the fraction of galaxies

<sup>1</sup> We convert accretion rate into luminosity assuming that the radiative efficiency equals the binding energy per unit mass of a particle in the last stable circular orbit. We associate the location of the last stable circular orbit to the spin of the MBHs, by self-consistently tracking the evolution of black hole spins throughout our calculations (Volonteri et al. 2005). We set 20% as the maximum value of the radiative efficiency, corresponding to a spin slightly below the theoretical limit for thin disc accretion (Thorne 1974).

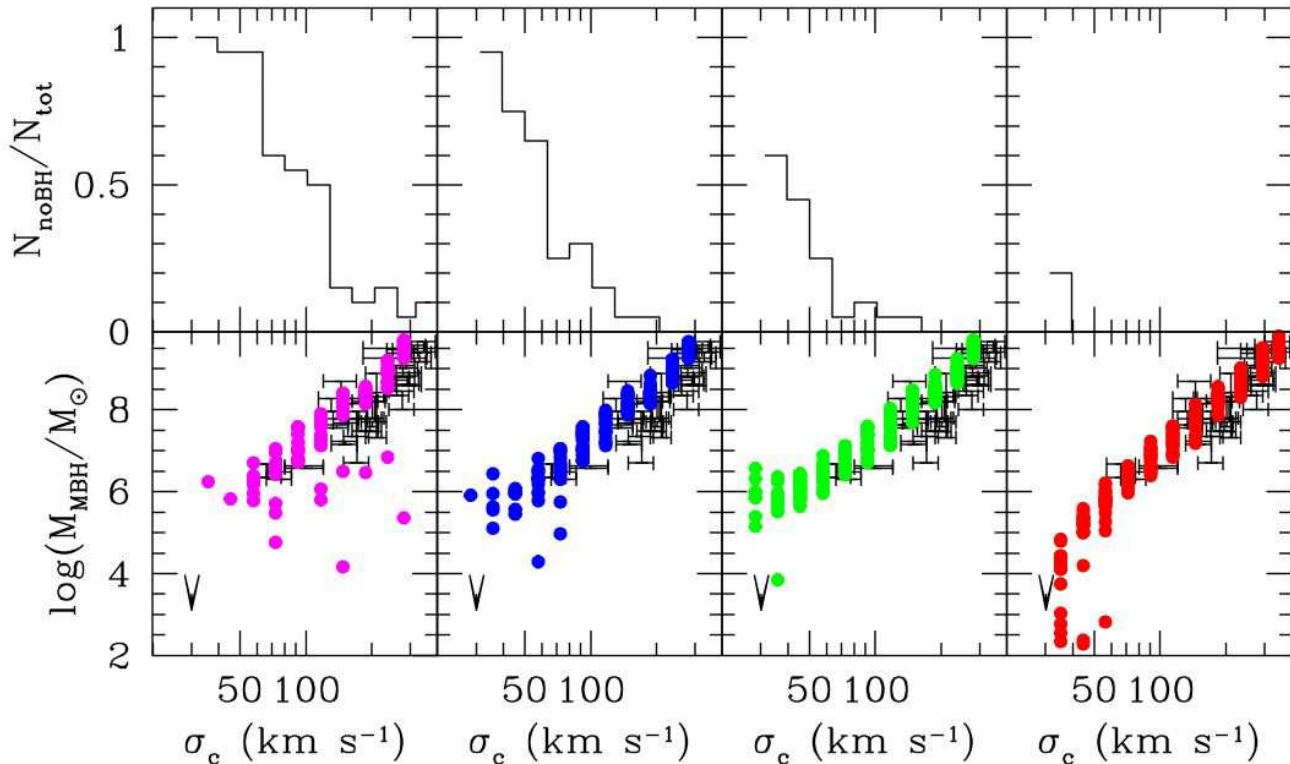


**Figure 3.** The  $M_{\text{bh}}$ –velocity dispersion ( $\sigma_c$ ) relation at  $z = 0$ . Every circle represents the central MBH in a halo of given  $\sigma_c$ . Observational data are marked by their quoted errorbars, both in  $\sigma_c$ , and in  $M_{\text{bh}}$  (Tremaine et al. 2002). Left to right panels:  $Q_c = 1.5$ ,  $Q_c = 2$ ,  $Q_c = 3$ , Population III star seeds. *Top panels:* fraction of galaxies at a given velocity dispersion which **do not** host a central MBH.

that **do not** host any massive black holes for different velocity dispersion bins. This shows that the fraction of galaxies without a MBH increases with decreasing halo masses at  $z = 0$ . A larger fraction of low mass halos are devoid of central black holes for lower seed formation efficiencies. Note that this is one of the key discriminants between our models and those seeded with Population III remnants. As shown in Fig. 3, there are practically no galaxies without central BHs for the Population III seeds.

It is interesting to note that our model predictions are in very good agreement with the recent HST ACS census of black holes in low mass galaxies in the Virgo cluster. Ferrarese et al. (2006); Wehner & Harris (2006) suggest that below a transition galaxy mass ( $\simeq 10^{10} M_\odot$ ) a central massive black hole seems to be replaced by a nuclear star cluster. Although no definite proof that Virgo dwarfs are indeed MBH-less, the above results imply that MBHs are more common in large galactic systems. Our models also indicate that a minimum velocity dispersion exists, below which the probability of finding a central object is very low.

We make quantitative predictions for the local occupation fraction of MBHs. Our model A predicts that below  $\sigma_c \approx 60 \text{ km s}^{-1}$  the probability of a galaxy hosting a MBH is negligible. With increasing MBH formation efficiencies, the minimum mass for a galaxy that hosts a MBH decreases,

and it drops below our simulation limits for model C. On the other hand, models based on lower mass Population III star remnant seeds, predict that massive black holes might be present even in low mass galaxies.

We note here that in our investigation we have not included any mechanism that could further lower the occupation fraction of MBHs (e.g., gravitational recoil, three-body MBH interactions). For any value of  $Q_c$  the occupation fraction computed above is therefore an upper limit.

Although there are degeneracies in our modeling (e.g., between the minimum redshift for BH formation and instability criterion), the BH occupation fraction, and the masses of the BHs in dwarf galaxies are the key diagnostics. In local observations, the clearest signatures of massive seeds compared to Population III remnants, would be a lower limit of order the typical mass of seeds (Fig. 2) to the mass of MBHs in galaxy centers, as shown in Fig. 3. An additional caveat worth mentioning is the possibility that a galaxy is devoid of a central MBH because of dynamical ejections (due to either the gravitational recoil or three-body scattering). The signatures of such dynamical interactions should be more prominent in dwarf galaxies, but ejected MBHs would leave observational signatures on their hosts (Gültekin et al. in prep.). On top of that, Schnittman (2007) and Volonteri (2007) agree in considering the recoil a minor correction to

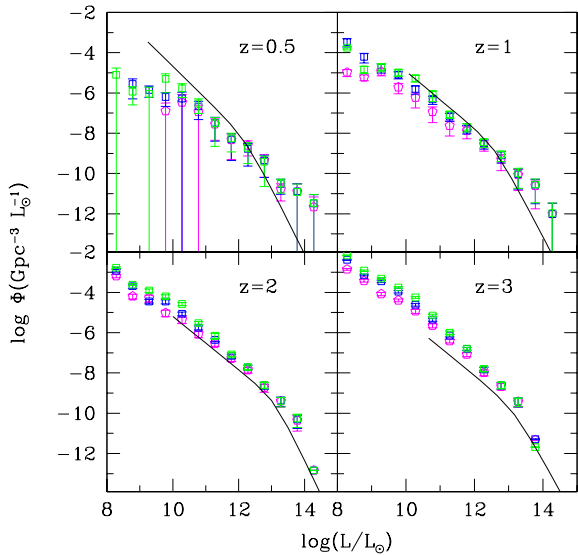


**Figure 4.** Bolometric luminosity functions at different redshifts. All 3 models match the observed bright end of the LF at high redshifts and predict a steep slope at the faint end down to  $z = 1$ . The 3 models are not really distinguishable with the LF. However at low redshifts, for instance at  $z = 0.5$ , all 3 models are significantly flatter at both high and low luminosities and do not adequately match the current data. As discussed in the text, the LF is strongly determined by the accretion prescription and what we see here is simply a reflection of that fact.

the overall distribution of the MBH population at low redshift (cfr. figure 4 in Volonteri 2007).

Additionally, as MBH seed formation requires halos with low angular momentum (low spin parameter), we envisage that low surface brightness, bulge-less galaxies with high spin parameters (i.e. large discs) are systems where MBH seed formation is less probable.<sup>2</sup> Furthermore, bulgeless galaxies are believed to preferentially have quieter merger histories and are unlikely to have experienced any major merger, which could have brought in a MBH from a companion galaxy. The (possible) absence of a MBH in M33 hence arises naturally (Merritt, Ferrarese & Joseph 2001; Gebhardt et al. 2001) in our model.

## 4.2 The luminosity function of accreting black holes

Turning to the global properties of the MBH population, as suggested by Yu & Tremaine (2002) the mass growth of the MBH population at  $z < 3$  is dominated by the mass accreted during the bright epoch of quasars, thus washing out most of the imprint of initial conditions. This is evident when we compute the luminosity function of AGN. Clearly the detailed shape of the predicted luminosity function depends most strongly on the accretion prescription used. With our assumption that the gas mass accreted during each merger

<sup>2</sup> This prediction is pertinent to all models relying on gravitational instabilities triggered in low spin parameter halos.

episode is proportional to  $V_c^5$ , we find that distinguishing between the various seed models is difficult. As shown in Fig. 4, all 3 models reproduce the bright end of the observed bolometric LF (Hopkins et al. 2007) at higher redshifts (marked as the solid curve in all the panels), and predict a fairly steep faint end that is as yet undetected. All models fare less well at low redshift, shown in particular at  $z = 0.5$ . This could be due to the fact that we have used a single accretion prescription to model growth through epochs. On the other hand, the decline in the available gas budget at low redshifts (since the bulk of the gas has been consumed by this epoch by star formation activity) likely changes the radiative efficiency of these systems. Besides, observations suggest a sharp decline in the number of actively accreting black holes at low redshifts across wave-lengths, produced most probably due to changes in the accretion flow as a result of change in the geometry of the nuclear regions of galaxies. In fact, all 3 of our models under-predict the slope at the faint end. There are three other effects that could cause this flattening of the LF at the faint end at low redshift for our models: (i) not having taken into account the fate of on-going merging and the fate of satellite galaxies; (ii) the number of realizations generated and tracked is insufficient for statistics, as evidenced by the systematically larger errorbars and (iii) more importantly, it is unclear if merger-driven accretion is indeed the trigger of BH fueling in the low redshift universe. We note that the 3 massive seed models and Population III seed model cannot be discriminated by the LF at high redshifts. Models B and C are also in agreement *viz-a-viz* the predicted BH mass function at  $z = 6$  (see Fig. 2), even assuming a very high radiative efficiency (up to 20%), while model A might need less severe assumptions, in particular for BH masses larger than  $10^7 M_\odot$ .

## 4.3 Comoving mass density of black holes

Since during the quasar epoch MBHs increase their mass by a large factor, signatures of the seed formation mechanisms are likely more evident at *earlier epochs*. We compare in Fig. 5 the integrated comoving mass density in MBHs to the expectations from Sołtan-type arguments (F. Haardt, private communication), assuming that quasars are powered by radiatively efficient flows (for details, see Yu & Tremaine 2002; Elvis et al. 2002; Marconi et al. 2004). While during and after the quasar epoch the mass densities in models A, B, and C differ by less than a factor of 2, at  $z > 3$  the differences become more pronounced.

A very efficient seed MBH formation scenario can lead to a very large BH density at high redshifts. For instance, the highest efficiency model C with  $Q_c = 3$ , the integrated MBH density at  $z = 10$  is already  $\sim 25\%$  of the density at  $z = 0$ . The plateau at  $z > 6$  is due to our choice of scaling the accreted mass with the  $z = 0$   $M_{\text{bh}}$ -velocity dispersion relation. Since in our models we let MBHs accrete a mass which scales with the fifth power of the circular velocity of the halo, the accreted mass is a small fraction of the MBH mass (see the discussion in Marulli et al. 2006), and the overall growth remains small, as long as the mass of the seed is larger than the accreted mass, which, in our assumed scaling, happens when the mass of the halo is below a few times  $10^{10} M_\odot$ . The comoving mass density, an integral constraint, is reasonably well determined out to  $z = 3$  but is

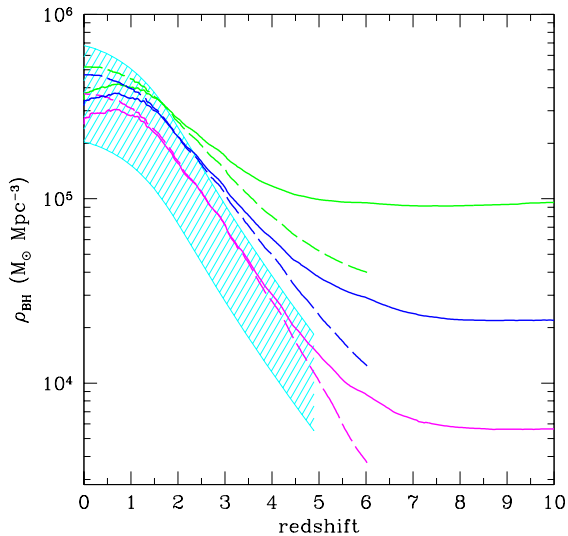


**Figure 5.** Integrated black hole mass density as a function of redshift. Solid lines: total mass density locked into nuclear black holes. Dashed lines: integrated mass density accreted by black holes. Models based on BH remnants of Population III stars (lowest curve),  $Q_c = 1.5$  (middle lower curve),  $Q_c = 2$  (middle upper curve),  $Q_c = 3$  (upper curve). Shaded area: constraints from Sołtan-type arguments, where we have varied the radiative efficiency from a lower limit of 6% (applicable to Schwarzschild MBHs, upper envelope of the shaded area), to about 20% (Wang et al. 2006). All 3 massive seed formation models are in comfortable agreement with the mass density obtained from integrating the optical luminosity functions of quasars.

poorly known at higher redshifts. All models appear to be satisfactory and consistent with current observational limits (shown as the shaded area).

#### 4.4 Black hole mass function at $z = 0$

One of the key diagnostics is the comparison of the measured and predicted BH mass function at  $z = 0$  for our 3 models. In Fig. 6, we show (from left to right, respectively) the mass function predicted by models A, B, C and Population III remnant seeds compared to that obtained from measurements. The histograms show the mass function obtained with our models (where the upper histogram includes all the black holes while the lower one only includes black holes found in central galaxies of halos in the merger-tree approach). The two lines are two different estimates of the observed black hole mass function. In the upper one, the measured velocity dispersion function for nearby late and early-type galaxies from the SDSS survey (Bernardi et al. 2003; Sheth et al. 2003) has been convolved with the measured  $M_{\text{BH}} - \sigma$  relation. We note here that the scatter in the  $M_{\text{bh}} - \sigma$  relation is not explicitly included in this treatment, however the inclusion of the scatter is likely to preferentially affect the high mass end of the BHMF, which provides stronger constraints on the accretion histories rather than the seed masses. It has been argued (e.g., Tundo et al. 2007; Bernardi et al. 2007; Lauer et al. 2007) that the BH mass function differs if the bulge mass is used instead of

the velocity dispersion in relating the BH mass to the host galaxy. Since our models do not trace the formation and growth of stellar bulges in detail, we are restricted to using the velocity dispersion in our analysis.

The lower dashed curve is an alternate theoretical estimate of the BH mass function derived using the Press-Schechter formalism from Jenkins et al. (2001) in conjunction with the observed  $M_{\text{BH}} - \sigma$  relation. Selecting only the central galaxies of halos in the merger-tree approach adopted here (lower histograms) is shown to be fairly equivalent to this analytical estimate, and this is clearly borne out as is evident from the plot. When we include black holes in satellite galaxies (upper histograms, cfr. the discussion in Volonteri, Haardt & Madau 2003) the predicted mass function moves towards the estimate based on SDSS galaxies. The higher efficiency models clearly produce more BHs. At higher redshifts, for instance at  $z = 6$ , the mass functions of active MBHs predicted by all models are in very good agreements in particular for BH masses larger than  $10^6 M_{\odot}$ , as it is the growth by accretion that dominates the evolution of the population. At the highest mass end ( $> 10^9 M_{\odot}$ ) model A lags behind models B and C, although we stress once again that our assumptions for the accretion process are very conservative.

The *relative* differences between models A, B, and C at the low-mass end of the mass function, however, are genuinely related to the MBH seeding mechanism (see also Figs. 3 and 5). In model A, simply, fewer galaxies host a MBH, hence reducing the overall number density of black holes. Although our simplified treatment does not allow robust quantitative predictions, the presence of a "bump" at  $z = 0$  in the MBH mass function at the characteristic mass that marks the peak of the seed mass function (cfr. Fig. 2) is a sign of highly efficient formation of massive seeds (i.e., much larger mass with respect, for instance, Population III remnants). The higher the efficiency of seed formation, the more pronounced is the bump (note that the bump is most prominent for model C). Since current measurements of MBH masses extend barely down to  $M_{\text{bh}} \sim 10^6 M_{\odot}$ , this feature cannot be observationally tested with present data but future campaigns, with the Giant Magellan Telescope or JWST, are likely to extend the mass function measurements to much lower black hole masses.

## 5 DISCUSSION AND IMPLICATIONS

In this paper, we have investigated the role that the choice of the initial seed black hole mass function at high redshift ( $z \sim 18$ ) plays in the determination of observed properties of local quiescent SMBHs. While the errors on mass determinations of local black holes are large at the present time, definite trends with host galaxy properties are observed. The tightest correlation appears to be between the BH mass and the velocity dispersion of the host spheroid. Starting with the ab-initio black hole seed mass function computed in the context of direct formation of central objects from the collapse of pre-galactic discs in high redshift halos, we follow the assembly history to late times using a Monte-Carlo merger tree approach. Key to our calculation of the evolution and build-up of mass is the prescription that we adopt for determining the precise mass gain during a merger. Mo-



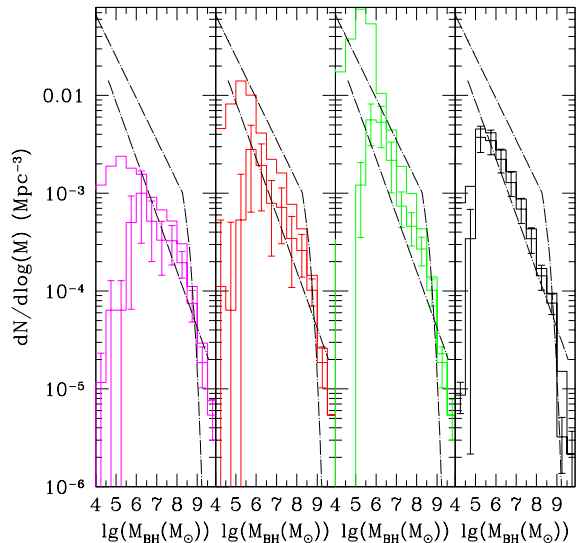


**Figure 6.** Mass function of black holes at  $z=0$ . Histograms represent the results of our models, including central galaxies only (lower histograms with errorbars), or including satellites in groups and clusters (upper histograms). Left panel:  $Q_c = 1.5$ , mid-left panel:  $Q_c = 2$ , mid-right panel:  $Q_c = 3$ , right panel: models based on BH remnants of Population III stars. Upper dashed line: mass function derived from combining the velocity dispersion function of Sloan galaxies (Sheth et al. 2003, where we have included the late-type galaxies extrapolation), and BH mass-velocity dispersion correlation (e.g., Tremaine et al. 2002). Lower dashed line: mass function derived using the Press-Schechter formalism from Jenkins et al. (2001) in conjunction with the  $M_{\text{BH}} - \sigma$  relation (Ferrarese 2002).

tivated by the phenomenological observation of  $M_{\text{BH}} \propto V_c^5$ , we assume that this proportionality carries over to the gas mass accreted in each step. With these prescriptions, a range of predictions can be made for the mass function of black holes at high and low  $z$ , and the integrated mass density of black holes, all of which are observationally determined. We evolve 3 models, designated model A, B and C which correspond to increasing efficiencies respectively for the formation of seeds at high redshift. These models are compared to one in which the seeds are remnants of Population III stars.

It is important to note here that one major uncertainty prevents us from making more concrete predictions: the unknown metal enrichment history of the Universe. Key to the implementation of our models is the choice of redshift at which massive seed formation is quenched. The direct seed formation channel described here ceases to operate once the Universe has been enriched by metals that have been synthesized after the first generation of stars have gone supernova. Once metals are available in the Inter-Galactic Medium gas cooling is much more efficient and hydrogen in either atomic or molecular form is no longer the key player. In this work we have assumed this transition redshift to be  $z = 15$ . The efficiency of MBH formation and the transition redshift are somehow degenerate (e.g., a model with  $Q = 1.5$  and enrichment redshift  $z = 12$  is halfway between model A and model B); if other constraints on this redshift were available we could considerably tighten our predictions.

Below we list our predictions and compare how they fare with respect to current observations. The models investigated here clearly differ in predictions at the low mass end of the black hole mass function. With future observational sensitivity in this domain, these models can be distinguished.

Our model for the formation of relatively high-mass black hole seeds in high- $z$  halos has direct influence on the black hole occupation fraction in galaxies at  $z = 0$ . This effect is more pronounced for low mass galaxies. We find that a significant fraction of low-mass galaxies might not host a nuclear black hole. This is in very good agreement with the shape of the  $M_{\text{bh}} - \sigma$  relation determined recently from an observational census (an HST ACS survey) of low mass galaxies in the Virgo cluster reported by Ferrarese et al. (2006).

The models studied here (with different black hole seed formation efficiency) are distinguishable at the low mass end of the BH mass function, while at the high mass end the effect of initial seeds appears to be sub-dominant. While current data in the low mass regime is scant (Barth et al. 2004; Greene & Ho 2007), future instruments and surveys are likely to probe this region of parameter space with significantly higher sensitivity.

All our models predict that low surface brightness, bulge-less galaxies with high spin parameters (i.e. large discs) are systems where MBH formation is least probable.

One of the key caveats of our picture is that it is unclear if the differences produced by different seed models on observables at  $z = 0$  might be compensated or masked by BH fueling modes at earlier epochs. There could be other channels for BH growth that dominate at low redshifts like minor mergers, dynamical instabilities, accretion of molecular clouds, tidal disruption of stars. The decreased importance of the merger driven scenario is patent from observations of low-redshift AGN, which are for the large majority hosted by undisturbed galaxies (e.g., Pierce et al. 2007, and references therein) in low-density environments (e.g., Li et al. 2006). However, the feasibility and efficiency of some alternative channels are still to be proven (for example, about the efficiency of feeding from large scale instabilities see discussion in King & Pringle 2007; Shlosman et al. 1989; Goodman 2003; Collin & Zahn 1999). In any event, while these additional channels for BH *growth* can modify the detailed shape of the mass function of MBHs, or of the luminosity function of quasars, they will not create a new MBH. The occupation fraction of MBHs (see figure 3) is therefore largely *independent* of the accretion mechanism and a true signature of the formation process.

To date, most theoretical models for the evolution of MBHs in galaxies do not include *how* MBHs form. This work is a first analysis of the observational signatures of massive black hole formation mechanisms in the low redshift universe, complementary to the investigation by Sesana et al. (2007), where the focus was on detection of seeds at the very early times where they form, via gravitational waves emitted during MBH mergers. We focus here on possible dynamical signatures that forming massive black hole seeds carries over to the local Universe. We believe that the signatures of seed formation mechanisms will be far more clear if considered jointly with the evolution of the spheroids that they host. The mass, and especially the frequency, of the

forming MBH seeds is a necessary input when investigating how the feedback from accretion onto MBHs influences the host galaxy, and is generally introduced in numerical models using extremely simplified, *ad hoc* prescriptions (e.g., Springel et al. 2005; Di Matteo et al. 2005; Hopkins et al. 2006; Croton et al. 2005; Cattaneo et al. 2006; Bower et al. 2006). Adopting more detailed models for black hole seed formation, as outlined here, can in principle strongly affect such results. For instance, Kauffmann et al. (2004) find that AGN activity is typically confined to galaxies with  $M > 10^{10} M_{\odot}$ . If we consider the occupation fraction of MBHs in such galaxies, we find that it differs by a large factor between models A and C, being of order 10% in the low efficiency model (at  $z \sim 1 - 4$ ) and 50% or higher in model C. Consequently, the possibility of AGN feedback and its effect on the host would be selective in the former case, or widespread in the latter case. Adopting sensible assumptions for the masses, and frequency of MBH seeds in models of galaxy formation is necessary if we want to understand the symbiotic growth of MBHs and their hosts.

## ACKNOWLEDGMENTS

PN and MV acknowledge the 2006 KITP program titled ‘The Physics of Galactic Nuclei’, supported in part by the National Science Foundation under Grant No. PHY99-07949.

## REFERENCES

- Abel T., Bryan G. L., Norman M. L., 2000, *ApJ*, 540, 39  
 Barger A. J., Cowie L. L., Capak P., Alexander D. M., Bauer F. E., Fernandez E., Brandt W. N., Garmire G. P., Hornschemeier A. E., 2003, *AJ*, 126, 632  
 Barger A. J., Cowie L. L., Mushotzky R. F., Yang Y., Wang W.-H., Steffen A. T., Capak P., 2005, *AJ*, 129, 578  
 Barth A. J., Ho L. C., Rutledge R. E., Sargent W. L. W., 2004, *ApJ*, 607, 90  
 Begelman M. C., Volonteri M., Rees M. J., 2006, *MNRAS*, 370, 289  
 Bernardi M., et al., 2003, *AJ*, 125, 1882  
 Bernardi M., Sheth R. K., Tundo E., Hyde J. B., 2007, *ApJ*, 660, 267  
 Bower R. G., Benson A. J., Malbon R., Helly J. C., Frenk C. S., Baugh C. M., Cole S., Lacey C. G., 2006, *MNRAS*, 370, 645  
 Bromley J. M., Somerville R. S., Fabian A. C., 2004, *MNRAS*, 350, 456  
 Bromm V., Coppi P. S., Larson R. B., 2002, *ApJ*, 564, 23  
 Bullock J. S., Dekel A., Kolatt T. S., Kravtsov A. V., Klypin A. A., Porciani C., Primack J. R., 2001, *ApJ*, 555, 240  
 Campanelli M., Lousto C., Zlochower Y., Merritt D., 2007a, *ApJ*, 659, L5  
 Campanelli M., Lousto C. O., Zlochower Y., Merritt D., 2007b, *Physical Review Letters*, 98, 231102  
 Carilli C. L., Kohno K., Kawabe R., Ohta K., Henkel C., Menten K. M., Yun M. S., Petric A., Tutui Y., 2002, *AJ*, 123, 1838  
 Cattaneo A., Dekel A., Devriendt J., Guiderdoni B., Blaizot J., 2006, *MNRAS*, 370, 1651  
 Cole S., Lacey C., 1996, *MNRAS*, 281, 716  
 Collin S., Zahn J. P., 1999, *A&A*, 344, 433  
 Cox P., Omont A., Djorgovski S. G., Bertoldi F., Pety J., Carilli C. L., Isaak K. G., Beelen A., McMahon R. G., Castro S., 2002, *A&A*, 387, 406  
 Croton D. J., et al., 2005, *MNRAS*, 356, 1155  
 Di Matteo T., Croft R. A. C., Springel V., Hernquist L., 2003, *ApJ*, 593, 56  
 Di Matteo T., Springel V., Hernquist L., 2005, *Nature*, 433, 604  
 Elvis M., Risaliti G., Zamorani G., 2002, *ApJ*, 565, L75  
 Fabian A. C., Iwasawa K., 1999, *MNRAS*, 303, L34  
 Fan X., et al., 2004, *AJ*, 128, 515  
 Fan X., et al., 2006, *AJ*, 131, 1203  
 Ferrarese L., 2002, *ApJ*, 578, 90  
 Ferrarese L., et al., 2006, *ApJS*, 164, 334  
 Ferrarese L., Merritt D., 2000, *ApJ*, 539, 9  
 Fitchett M. J., 1983, *MNRAS*, 203, 1049  
 Gebhardt K., et al., 2000, *AJ*, 119, 1157  
 González J. A., Sperhake U., Brüggemann B., Hannam M., Husa S., 2007, *Physical Review Letters*, 98, 091101  
 Goodman J., 2003, *MNRAS*, 339, 937  
 Greene J. E., Ho L. C., 2007, *ArXiv e-prints*, 0707.2617  
 Haehnelt M. G., Natarajan P., Rees M. J., 1998, *MNRAS*, 300, 817  
 Haiman Z., Loeb A., 1998, *ApJ*, 503, 505  
 Hasinger G., et al., 2001, *A&A*, 365, L45  
 Herrmann F., Hinder I., Shoemaker D. M., Laguna P., Matzner R. A., 2007, *ArXiv e-prints*, 0706.2541  
 Hopkins P. F., Hernquist L., Cox T. J., Di Matteo T., Robertson B., Springel V., 2005a, *ApJ*, 630, 716  
 Hopkins P. F., Hernquist L., Cox T. J., Di Matteo T., Robertson B., Springel V., 2005b, *ApJ*, 632, 81  
 Hopkins P. F., Hernquist L., Cox T. J., Di Matteo T., Robertson B., Springel V., 2006, *ApJS*, 163, 1  
 Hopkins P. F., Richards G. T., Hernquist L., 2007, *ApJ*, 654, 731  
 Jenkins A., Frenk C. S., White S. D. M., Colberg J. M., Cole S., Evrard A. E., Couchman H. M. P., Yoshida N., 2001, *MNRAS*, 321, 372  
 Kauffmann G., Haehnelt M., 2000, *MNRAS*, 311, 576  
 Kauffmann G., Haehnelt M. G., 2002, *MNRAS*, 332, 529  
 Kauffmann G., White S. D. M., Heckman T. M., Ménard B., Brinchmann J., Charlot S., Tremonti C., Brinkmann J., 2004, *MNRAS*, 353, 713  
 King A., 2003, *ApJ*, 596, L27  
 King A. R., Pringle J. E., 2007, *MNRAS*, 377, L25  
 Koushiappas S. M., Bullock J. S., Dekel A., 2004, *MNRAS*, 354, 292  
 Lacey C., Cole S., 1993, *MNRAS*, 262, 627  
 Lauer T. R., et al., 2007, *ArXiv e-prints*, 0705.4103  
 Li C., Kauffmann G., Wang L., White S. D. M., Heckman T. M., Jing Y. P., 2006, *MNRAS*, 373, 457  
 Lodato G., Natarajan P., 2006, *MNRAS*, 371, 1813  
 Lodato G., Natarajan P., 2007, *MNRAS*, 377, L64  
 Lodato G., Rice W. K. M., 2004, *MNRAS*, 351, 630  
 Lodato G., Rice W. K. M., 2005, *MNRAS*, 358, 1489  
 Lynden-Bell D., 1969, *Nature*, 223, 690  
 Madau P., Rees M. J., 2001, *ApJ*, 551, L27

- Marconi A., Risaliti G., Gilli R., Hunt L. K., Maiolino R., Salvati M., 2004, *MNRAS*, 351, 169
- Martínez-Sansigre A., Rawlings S., Lacy M., Fadda D., Marleau F. R., Simpson C., Willott C. J., Jarvis M. J., 2005, *Nature*, 436, 666
- Marulli F., Crociani D., Volonteri M., Branchini E., Moscardini L., 2006, *MNRAS*, 368, 1269
- Mo H. J., Mao S., White S. D. M., 1998, *MNRAS*, 295, 319
- Mushotzky R. F., Cowie L. L., Barger A. J., Arnaud K. A., 2000, *Nature*, 404, 459
- Omont A., Cox P., Bertoldi F., McMahon R. G., Carilli C., Isaak K. G., 2001, *A&A*, 374, 371
- Page L., et al., 2003, *ApJS*, 148, 233
- Pierce C. M., Lotz J. M., Laird E. S., Lin L., Nandra K., Primack J. R., Faber S. M., Barmby P., Park S. Q., Willner S. P., Gwyn S., Koo D. C., Coil A. L., Cooper M. C., Georgakakis A., Koekemoer A. M., Noeske K. G., Weiner B. J., Willmer C. N. A., 2007, *ApJ*, 660, L19
- Press W. H., Schechter P., 1974, *ApJ*, 187, 425
- Redmount I. H., Rees M. J., 1989, *Comments on Astrophysics*, 14, 165
- Rice W. K. M., Lodato G., Armitage P. J., 2005, *MNRAS*, 364, L56
- Schnittman, J. D. 2007, *ApJ*, 667, L133
- Sesana A., Volonteri M., Haardt F., 2007, *MNRAS*, 377, 1711
- Shapiro S. L., Shibata M., 2002, *ApJ*, 577, 904
- Sheth R. K., et al., 2003, *ApJ*, 594, 225
- Shlosman I., Frank J., Begelman M. C., 1989, *Nature*, 338, 45
- Silk J., Rees M. J., 1998, *A&A*, 331, L1
- Spergel D. N., et al., 2003, *ApJS*, 148, 175
- Springel V., White S. D. M., Jenkins A., Frenk C. S., Yoshida N., Gao L., Navarro J., Thacker R., Croton D., Helly J., Peacock J. A., Cole S., Thomas P., Couchman H., Evrard A., Colberg J., Pearce F., 2005, *Nature*, 435, 629
- Thompson T. A., Quataert E., Murray N., 2005, *ApJ*, 630, 167
- Thorne K. S., 1974, *ApJ*, 191, 507
- Toomre A., 1964, *ApJ*, 139, 1217
- Tremaine S., et al., 2002, *ApJ*, 574, 740
- Tundo E., Bernardi M., Hyde J. B., Sheth R. K., Pizzella A., 2007, *ApJ*, 663, 53
- van den Bosch F. C., Abel T., Croft R. A. C., Hernquist L., White S. D. M., 2002, *ApJ*, 576, 21
- Volonteri M., 2007, *ApJ*, 663, L5
- Volonteri M., Haardt F., Madau P., 2003, *ApJ*, 582, 559
- Volonteri M., Madau P., Quataert E., Rees M. J., 2005, *ApJ*, 620, 69
- Volonteri M., Rees M. J., 2005, *ApJ*, 633, 624
- Volonteri M., Salvaterra R., Haardt F., 2006, *MNRAS*, 373, 121
- Volonteri M. e. a., 2007, in preparation
- Walter F., Bertoldi F., Carilli C., Cox P., Lo K. Y., Neri R., Fan X., Omont A., Strauss M. A., Menten K. M., 2003, *Nature*, 424, 406
- Warren M. S., Quinn P. J., Salmon J. K., Zurek W. H., 1992, *ApJ*, 399, 405
- Wehner E. H., Harris W. E., 2006, *ApJ*, 644, L17
- Worsley M. A., Fabian A. C., Bauer F. E., Alexander D. M., Hasinger G., Mateos S., Brunner H., Brandt W. N., Schneider D. P., 2005, *MNRAS*, 357, 1281
- Wyithe J. S. B., Loeb A., 2002, *ApJ*, 581, 886
- Yu Q., Tremaine S., 2002, *MNRAS*, 335, 965